

# Geophysical Research Letters

## RESEARCH LETTER

10.1029/2018GL081215

### Key Points:

- Understanding atmospheric CO<sub>2</sub> across the Cretaceous-Paleogene boundary has been limited due to deficiencies in existing records
- Our study highlights the utility of a proxy based on leaf gas exchange principles
- We record a small transient rise in atmospheric CO<sub>2</sub> that is more in line with modeled estimates of both Deccan volcanism and a bolide impact

### Supporting Information:

- Supporting Information S1
- Data Set S1

### Correspondence to:

J. N. Milligan,  
joseph\_milligan@baylor.edu

### Citation:

Milligan, J. N., Royer, D. L., Franks, P. J., Upchurch, G. R., & McKee, M. L. (2019). No evidence for a large atmospheric CO<sub>2</sub> spike across the Cretaceous-Paleogene boundary. *Geophysical Research Letters*, *46*, 3462–3472. <https://doi.org/10.1029/2018GL081215>

Received 20 JUN 2018

Accepted 3 MAR 2019

Accepted article online 7 MAR 2019

Published online 29 MAR 2019

## No Evidence for a Large Atmospheric CO<sub>2</sub> Spike Across the Cretaceous-Paleogene Boundary

Joseph N. Milligan<sup>1,2</sup> , Dana L. Royer<sup>1</sup> , Peter J. Franks<sup>3</sup> , Garland R. Upchurch<sup>4</sup> , and Melissa L. McKee<sup>1</sup>

<sup>1</sup>Department of Earth and Environmental Sciences, Wesleyan University, Middletown, CT, USA, <sup>2</sup>Department of Geology, Baylor University, Waco, TX, USA, <sup>3</sup>School of Life and Environmental Sciences, University of Sydney, Sydney, New South Wales, Australia, <sup>4</sup>Department of Biology, Texas State University, San Marcos, TX, USA

**Abstract** Currently, there is only one paleo-CO<sub>2</sub> record from plant macrofossils that has sufficient stratigraphic resolution to potentially capture a transient spike related to rapid carbon release at the Cretaceous-Paleogene (K-Pg) boundary. Unfortunately, the associated measurements of stomatal index are off-calibration, leading to a qualitative interpretation of >2,300-ppm CO<sub>2</sub>. Here we reevaluate this record with a paleo-CO<sub>2</sub> proxy based on leaf gas exchange principles. We also test the proxy with three living species grown at 500- and 1,000-ppm CO<sub>2</sub>, including the nearest living relative of the K-Pg fern, and find a mean error rate of ~22%, which is comparable to other leading paleo-CO<sub>2</sub> proxies. Our fossils record a ~250-ppm increase in CO<sub>2</sub> across the K-Pg boundary from ~625 to ~875 ppm. A small CO<sub>2</sub> spike associated with the end-Cretaceous mass extinction is consistent with many temperature records and with carbon cycle modeling of Deccan volcanism and the meteorite impact.

**Plain Language Summary** Currently, there is only one paleo-CO<sub>2</sub> record close enough to the Cretaceous-Paleogene (K-Pg) boundary to record a rapid release in atmospheric CO<sub>2</sub>, a greenhouse gas. This record is based on the stomatal frequencies of fern fossils at the K-Pg boundary and *Ginkgo* fossils before and after the boundary. Unfortunately, due to deficiencies with the method, the CO<sub>2</sub> inferences are only qualitative. Here we look at the same fossils with a proxy based on leaf gas exchange principles (i.e., photosynthesis). We first test the proxy with three living species grown at 500- and 1,000-ppm CO<sub>2</sub>, including the nearest living relative of the K-Pg fern, and find a comparable accuracy to other quantitative paleo-CO<sub>2</sub> proxies. The fossils record a modest ~250-ppm increase in CO<sub>2</sub> across the K-Pg boundary. These estimates are consistent with most temperature records and with carbon cycle modeling of Deccan volcanism and the meteorite impact.

### 1. Introduction

The Cretaceous–Paleogene (K-Pg) boundary ~66 Ma marks one of the largest mass extinctions in Earth's history (Alroy, 2008; Brusatte et al., 2015; McElwain & Punyasena, 2007; Raup & Sepkoski, 1982). The concentration of atmospheric CO<sub>2</sub> may have risen abruptly at this time, contributing to the biological upheaval (Beerling et al., 2002). Removal of an instantaneous release of CO<sub>2</sub> to the atmosphere typically requires up to 100–200 kyrs, following exponential decay due to silicate weathering (Archer, 2005; Colbourn et al., 2015; Schaller et al., 2011; Zeebe & Zachos, 2013). Adequate constraints on atmospheric CO<sub>2</sub> from proxy records during this critical period have been missing, mostly because of a lack in sufficient stratigraphic resolution to definitively identify individual records occurring <100 kyrs after the extinction event. This is because either the stratigraphic section is too coarse to resolve 100 kyrs of time (Steinthorsdottir et al., 2016) or because definitive markers of the boundary (e.g., iridium spike, presence of microspherules) are missing (Huang et al., 2013; Nordt et al., 2003; Zhang et al., 2018).

One exception is the study of Beerling et al. (2002), who used stomatal indices (SI, stomatal density normalized by the number of epidermal cells) to estimate CO<sub>2</sub> from fern macrofossils (aff. *Stenochlaena*) that occur 5–25 cm above the K-Pg boundary in the Raton Basin, New Mexico. In this stratigraphic section, the K-Pg boundary is identified by an iridium spike and shocked quartz, and the fossils come from sediments that contain, and lie directly above, the fern spore spike. This fern spike is present across the globe (Vajda et al., 2001) and likely occurred within 10<sup>3</sup> years after the K-Pg boundary (Clyde et al., 2016). Thus, the aff. *Stenochlaena* fossils should record any transient rise in atmospheric CO<sub>2</sub> associated with the Chicxulub impact and K-Pg

boundary. Indeed, the fossils likely capture close to the peak in CO<sub>2</sub> change because after an instantaneous release, CO<sub>2</sub> will remain significantly elevated for hundreds of years (Solomon et al., 2009; Zeebe, 2013). Unfortunately, the measured stomatal indices fall well below the present-day calibration of *S. palustris*, leading Beerling et al. (2002) to interpret a CO<sub>2</sub> concentration that exceeded the calibrated space (>2,300 ppm), considerably higher than latest Cretaceous and earliest Paleocene CO<sub>2</sub> values of ~350–550 ppm inferred from *Ginkgo* fossils (Beerling et al., 2002, 2009). The Beerling et al. (2002) study thus suggests a very large, but poorly constrained, CO<sub>2</sub> pulse.

Leaf gas exchange models are an alternative to stomatal density (SD) and SI proxies for estimating paleo-CO<sub>2</sub> concentration (Franks et al., 2014; Konrad et al., 2008, 2017). The model developed by Franks et al. (2014) depends on the well-established relationship between the rate of CO<sub>2</sub> assimilation of plants ( $A$ ), leaf conductance to CO<sub>2</sub> ( $g_{\text{ctot}}$ ), and the difference between atmospheric ( $c_a$ ) and leaf intercellular CO<sub>2</sub> ( $c_i$ ; Farquhar & Sharkey, 1982):

$$A = g_{\text{ctot}}(c_a - c_i) \quad (1)$$

Equation (1) can be rearranged to solve for atmospheric CO<sub>2</sub> (equation (2)). The three input variables needed are the average assimilation rate (determined from a nearest living relative), average total leaf conductance (determined largely from SD and stomatal size measured on the fossil), and average  $c_i/c_a$  (determined from the fossil leaf and air carbon isotopic composition combined with knowledge of the fractionation process; Franks et al., 2014):

$$c_a = \frac{A}{g_{\text{ctot}}(1 - c_i/c_a)} \quad (2)$$

The model has been used to reconstruct CO<sub>2</sub> during the Phanerozoic (Franks et al., 2014), including the late Paleozoic (Montañez et al., 2016), middle Cretaceous (Richey et al., 2018), Late Cretaceous (Martínez et al., 2018), early Paleocene (Kowalczyk et al., 2018), middle Eocene (Maxbauer et al., 2014; Wolfe et al., 2017), Oligocene-Miocene boundary (Reichgelt et al., 2016; Tesfamichael et al., 2017) and early Miocene (Londoño et al., 2018).

Leaf gas exchange models provide at least five crucial advantages over other stomatal approaches: (1) They are based mechanistically on physiological principles, not empirical, species-specific calibrations; (2) measurements of SD, a component of  $g_{\text{ctot}}$ , are typically more reliable and easier to make than SI because epidermal cells can be difficult to count (Barclay & Wing, 2016); (3) they are less sensitive to the saturating effect that can limit other stomatal methods to <500–1,000 ppm CO<sub>2</sub> (e.g., Doria et al., 2011); (4) they can be applied to most subaerial leaves from C<sub>3</sub> species, regardless of age or taxonomy; and (5) they are not restricted to species whose SD or SI is sensitive to CO<sub>2</sub>, because the models have multiple physiological inputs with well-understood sensitivities to CO<sub>2</sub>. Importantly, these gas exchange methods open up much of the paleobotanical record for quantitative CO<sub>2</sub> inference, not just to fossil taxa that are still living today. While the Franks et al. (2014) model shows promise, more extensive testing will improve confidence in the CO<sub>2</sub> estimates. Specifically, model validation with extant species has been limited to mostly angiosperms and a few gymnosperms, neglecting major clades such as ferns and lycophytes. Additionally, the model has been tested at elevated CO<sub>2</sub> on only a few species (Franks et al., 2014; Londoño et al., 2018).

Here we test the model using growth chamber experiments at elevated CO<sub>2</sub> (500 and 1,000 ppm) for two ferns (*Osmundastrum cinnamomeum* (L.) C. Presl and a close living relative to the K-Pg fern, *Stenochlaena palustris* (Burm.f.) Bedd.), and one conifer (*Cedrus deodara* (Roxb.) Loud). We then use the same fossils of aff. *Stenochlaena* and *Ginkgo* from Beerling et al. (2002) to reevaluate atmospheric CO<sub>2</sub> across the K-Pg boundary using the gas exchange model of Franks et al. (2014).

## 2. Materials and Methods

For detailed methods and all data, see the supporting information.

### 2.1. Growth Chamber Experiments

All plants were potted with Premier Horticulture “Pro-mix” Bx with Mycorise and grown in two Conviron E7/2 growth chambers. Plants were watered to field capacity daily and given Scotts all-purpose flower and

vegetable fertilizer (10-10-10) every 2 months. The chamber conditions were set to a 17-hr photoperiod with a 30-min simulated dawn and dusk. Temperature was  $25 \pm 0.2$  °C ( $1\sigma$ ) during the day and  $20 \pm 1$  °C ( $1\sigma$ ) at night. The relative humidity was  $84 \pm 5\%$  ( $1\sigma$ ) and the CO<sub>2</sub> concentration was either  $500 \pm 25$  ( $1\sigma$ ) or  $1,000 \pm 15$  ( $1\sigma$ ) ppm. Growth light levels (photosynthetically active radiation) varied between 100 and  $500 \mu\text{mol}\cdot\text{m}^{-2}\cdot\text{s}^{-1}$  depending on plant height. Plants were rotated between the two chambers every 2 weeks to negate any chamber effects (e.g., Porter et al., 2015).

## 2.2. Fossil Leaves

The fossils come from Beerling et al. (2002). The aff. *Stenochlaena* fossils were collected at the Clear Creek South locality in the Raton Basin, New Mexico (Wolfe & Upchurch, 1987). The fossils represent an extinct (and currently unnamed) genus related to *Stenochlaena* (Wolfe & Upchurch, 1987), with identification based on venation, tooth and frond architecture, and stomatal anatomy, especially maceration-resistant cutin lamellae on the guard cells (Beerling et al., 2002; Wolfe & Upchurch, 1987). The stratigraphic interval containing the fern fossils includes the top of the fern spore spike and the overlying level where dicot pollen returns to dominance.

The latest Cretaceous and earliest Paleocene *Ginkgo adiantoides* fossils were obtained by loan from the Denver Museum of Nature and Science and the Yale Peabody Museum, respectively. The Cretaceous fossils come from the Hell Creek Formation in the Williston Basin of North Dakota (Denver Museum of Nature and Science site 566), 33.5 m below the K-Pg boundary (Johnson, 2002). Based on constraints from geochronology, magnetostratigraphy, and sedimentation rates, Hicks et al. (2002) consider the locality 0.5 Myr older than the K-Pg boundary. The early Paleocene fossils come from the Fort Union Formation in the Bighorn Basin of Wyoming (Yale Peabody Museum site 7659), 4 m above the K-Pg boundary; based on sedimentation rates, Wing et al. (1995) interpret the site to postdate the K-Pg boundary by 0.5 Myr. We assume a K-Pg boundary age of 66 Ma (Gradstein et al., 2012; Renne et al., 2013).

## 2.3. Leaf Gas Exchange Model

The Franks et al. (2014) leaf gas exchange model has 16 inputs that are used to calculate the average assimilation rate, total leaf conductance, and  $c_i/c_a$  (equation (2)). When possible, we measured the inputs directly, including SD, stomatal pore length, single guard cell width, and leaf  $\delta^{13}\text{C}$  (Table S1). For living plants, the assimilation rate,  $A$ , and operational stomatal conductance to CO<sub>2</sub>,  $g_{c(\text{op})}$ , were also measured with a LI-COR 6400 portable photosynthesis system. These measurements were made under environmental conditions identical (or nearly identical) to the growth chamber environment. Leaves first equilibrated inside the leaf chamber for 10 to 30 min. All reported results are means of the most stable individual measurements (typically <5% variance across measurements).

For the fossil leaves, nearest living relatives were used to assign taxon-specific values of  $A_0$  (assimilation rate at a known CO<sub>2</sub> concentration) and  $g_{c(\text{op})}/g_{c(\text{max})}$  (ratio of operational to maximum stomatal conductance to CO<sub>2</sub>). For aff. *Stenochlaena*, values come from *S. palustris* reported here; for *G. adiantoides*, values come from field-grown *G. biloba* at ~400 ppm CO<sub>2</sub> (Kowalczyk et al., 2018). For other inputs not directly measured, we used the recommended values from Franks et al. (2014) or appropriate values from the literature (see Data Set S1). To solve for atmospheric CO<sub>2</sub>, we use the Kowalczyk et al. (2018) code written in R (v.3.4.4; R Core Team, 2018).

As with the Beerling et al. (2002) study, our atmospheric CO<sub>2</sub> reconstruction comes from two different species at three different localities. Because this potentially introduces species and environmental effects, we performed a sensitivity analysis by estimating CO<sub>2</sub> after sequentially varying each input parameter across a range typical for C<sub>3</sub> plants. Consistent with previous work (Kowalczyk et al., 2018; Maxbauer et al., 2014; McElwain et al., 2016) we find that among the inputs that cannot be measured directly on fossils, changes in  $A_0$  and  $g_{c(\text{op})}/g_{c(\text{max})}$  have the biggest impact on estimated CO<sub>2</sub> (Figure S16). As such, we explored how different value choices for these inputs may affect our CO<sub>2</sub> estimates. For example, because a one-step change in CO<sub>2</sub> may not induce the same physiological response as a slow-and-steady CO<sub>2</sub> increase over geological time, we evaluated the model both with the measured physiological inputs (discussed earlier) and generic values recommended by Franks et al. (2014; Table S2).

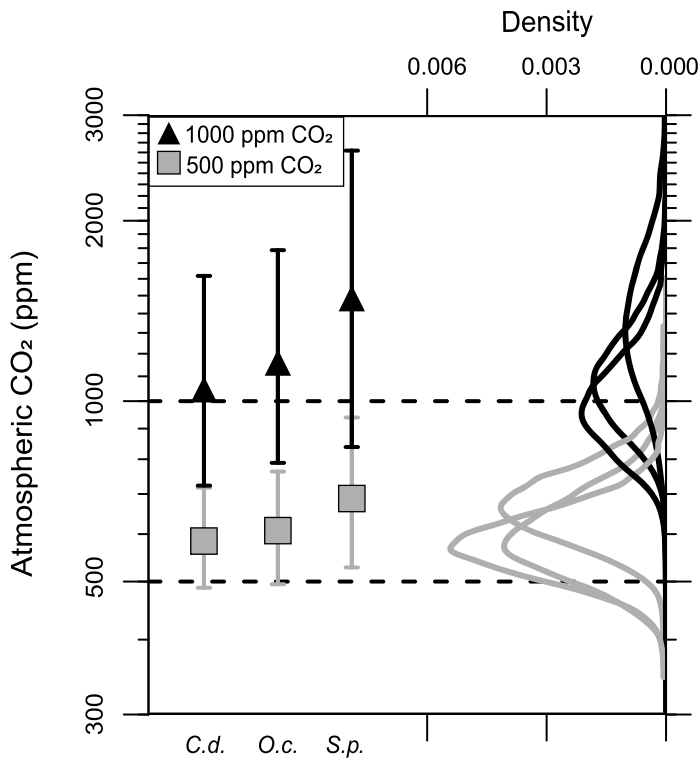


**Figure 1.** Atmospheric CO<sub>2</sub> estimates and probability density function using the leaf gas exchange model of Franks et al. (2014) with *Cedrus deodara* (*C.d.*), *Osmundastrum cinnamomeum* (*O.c.*), and *Stenochlaena palustris* (*S.p.*), grown at two CO<sub>2</sub> treatments (500- and 1,000-ppm CO<sub>2</sub>). Dotted lines represent the target CO<sub>2</sub> concentrations. Estimates are the median and 95% confidence interval.

We note that the Franks et al. (2014) leaf gas exchange model is based on leaf temperature, not air temperature. Both theory (Michaletz et al., 2015, 2016) and observations (Helliker & Richter, 2008; Song et al., 2011) indicate that the control of leaf gas exchange leads to relatively stable assimilation-weighted leaf temperatures (~19–25 °C from temperate to tropical regions; that is, thermoregulation). Thus, despite significant changes (e.g., several degrees) in global mean air temperature, as often observed across the K-Pg boundary, daytime leaf temperature during the growing season should stay relatively constant. If instead leaf temperature did vary substantially, it could have mixed effects on many model inputs ( $A$ ,  $g_{c(op)}/g_{c(max)}$ ,  $SD$ , stomatal size,  $c_i/c_a$ ); for example, an increase in  $A$  with no changes to other inputs will cause an equally proportional increase in estimated CO<sub>2</sub> (Figure S16B). While assimilation rates can increase with leaf temperature within seconds to hours (e.g., Berry & Björkman, 1980); C<sub>3</sub> plants generally exhibit stable assimilation rates when acclimated to a range of growth temperatures (i.e., temperature homeostasis of photosynthesis, Yamori et al., 2014). With regard to the Franks et al. (2014) model, tests on six species grown at 20 and 28 °C air temperature show only a mild effect on the ability of the model to estimate CO<sub>2</sub> (Royer et al., 2018). For these reasons, we argue that changes in mean global temperature probably have little impact on the reliability of our CO<sub>2</sub> reconstructions.

## 2.4. Statistics

A one-sample Kolmogorov-Smirnov test identified that most of our inputs did not have normal distributions (Data Set S1). Thus, for our experiments, we used a two-sample Kolmogorov-Smirnov test to test for differences between CO<sub>2</sub> treatments in the inputs. All analyses were done within R and performed at the plant level.

## 3. Results and Discussion

### 3.1. Growth Chamber Experiments

The median CO<sub>2</sub> estimates for the three living species in the 500 ppm CO<sub>2</sub> treatment range from 584–686 ppm, and in the 1,000 ppm treatment from 1,016–1,442 ppm (Figure 1 and Table S2). Across all species, the 500 and 1,000 ppm CO<sub>2</sub> treatments have a mean error rate [ $(\text{estimated CO}_2 - \text{observed CO}_2) / (\text{observed CO}_2)$ ] of ~25% and ~19%, respectively. This is higher than elevated CO<sub>2</sub> experiments of *Wollemia nobilis* at 480 and 1,270 ppm (7%; Franks et al., 2014), but is comparable to other paleo-CO<sub>2</sub> proxies at present-day CO<sub>2</sub> such as alkenones (12.4%; Pagani, 2002), boron isotopes (8.2%; Henehan et al., 2013; Hönisch & Hemming, 2005), and pedogenic carbonates (67%; Ekart et al., 1999). Additionally, the precision of estimates within this study are comparable or better than other paleo-CO<sub>2</sub> proxies, especially at elevated CO<sub>2</sub> (Beerling et al., 2009; Montañez et al., 2011; Royer, 2014). Using the generic values recommended by Franks et al. (2014) for  $A_0$  and  $g_{c(op)}/g_{c(max)}$ , median CO<sub>2</sub> estimates increase for *S. palustris* and *O. cinnamomeum* while decreasing for *C. deodara*, with a mean error rate of 44% and 21% for the 500 and 1,000 ppm CO<sub>2</sub> treatments (Table S2). Note, however, that the generic values recommended by Franks et al. (2014) were obtained for field conditions which may differ slightly from growth chambers. Plants in growth chambers typically experience lower light and higher humidity, which affect  $A_0$  and  $g_{c(op)}/g_{c(max)}$  via  $g_{c(op)}$ .

*O. cinnamomeum* and *C. deodara* show no significant differences to CO<sub>2</sub> in  $SD$ , guard cell length, stomatal pore length, single guard cell width, and  $g_{c(op)}/g_{c(max)}$  ( $P > 0.05$ ), but both have significantly higher  $A$  at 1,000 ppm CO<sub>2</sub> ( $P = 0.03$ ;  $P = 0.02$ ; Figure 2).  $SD$  in *S. palustris* declines significantly by 21% at high growth CO<sub>2</sub> ( $P = 0.048$ ), but with no significant change in guard cell length, stomatal pore length, or guard cell width ( $P > 0.05$ ). *C. deodara* and *S. palustris* exhibit a significant increase in  $c_i/c_a$  at elevated CO<sub>2</sub> ( $P = 0.004$ ;  $P = 0.048$ ), while *O. cinnamomeum* does not.

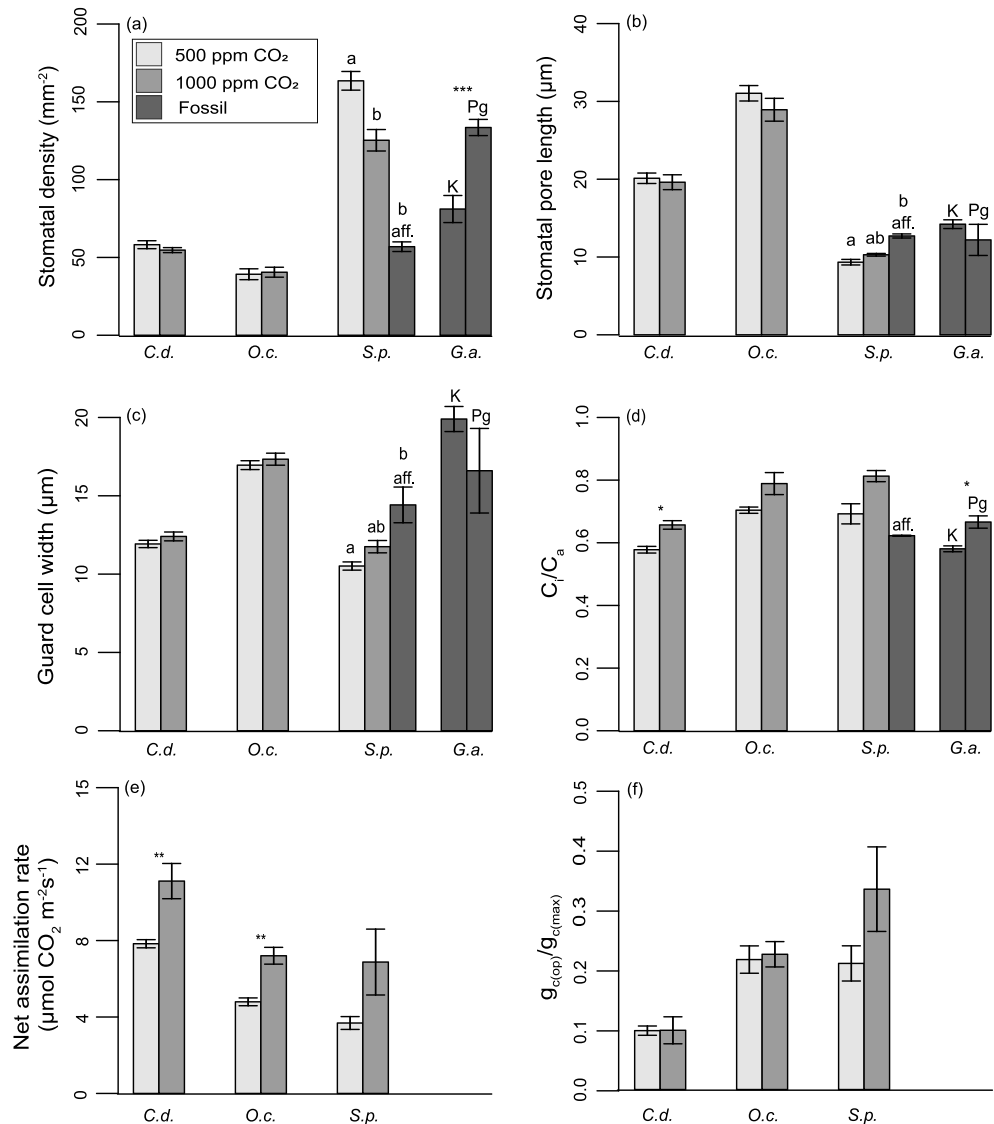


**Figure 2.** Measured inputs for *Cedrus deodara* (C.d.), *Osmundastrum cinnamomeum* (O.c.), and *Stenochlaena palustris* (S.p.) grown at two CO<sub>2</sub> concentrations (500 and 1,000 ppm) and fossil *Ginkgo adiantoides* (G.a.) and aff. *Stenochlaena*. Abbreviations: K, Cretaceous; Pg, Paleogene. For multiple comparisons different letters indicate significantly different values at the 0.05 level. \*  $P \leq 0.05$ , \*\*  $P \leq 0.01$ , \*\*\*  $P \leq 0.001$ .

The disparate physiological and morphological responses to CO<sub>2</sub> highlight an advantage of leaf gas exchange proxies over other stomatal proxies. If SD or SI does not respond to CO<sub>2</sub>, then by definition the SD and SI methods cannot be used (see Reichgelt et al., 2016). For leaf gas exchange models, this is not necessarily true if other inputs do respond to CO<sub>2</sub>. This is in fact the case with *O. cinnamomeum* and *C. deodara*, which produced reasonable CO<sub>2</sub> estimates for both treatments despite no changes in SD. Part of the issue with the other stomatal proxies is that they depend on a calibrated response, and the time scale associated with these responses (typically months to years) may not be sufficiently long, especially at higher-than-present CO<sub>2</sub> concentrations (Royer, 2001; see multiyear response from Hincke et al., 2016).

### 3.2. K-Pg Boundary CO<sub>2</sub>

The leaf gas exchange estimates of CO<sub>2</sub> from *G. adiantoides* are similar for the Late Cretaceous (66.5 Ma; 624 ppm; 95% confidence interval 454–882 ppm) and early Paleocene (65.5 Ma; 630 ppm; 95% confidence interval 408–1,181 ppm; Figure 3 and Table S2). The larger uncertainty with the Paleocene estimate is mostly due to having to model both stomatal pore length and single guard cell width because we were unable to

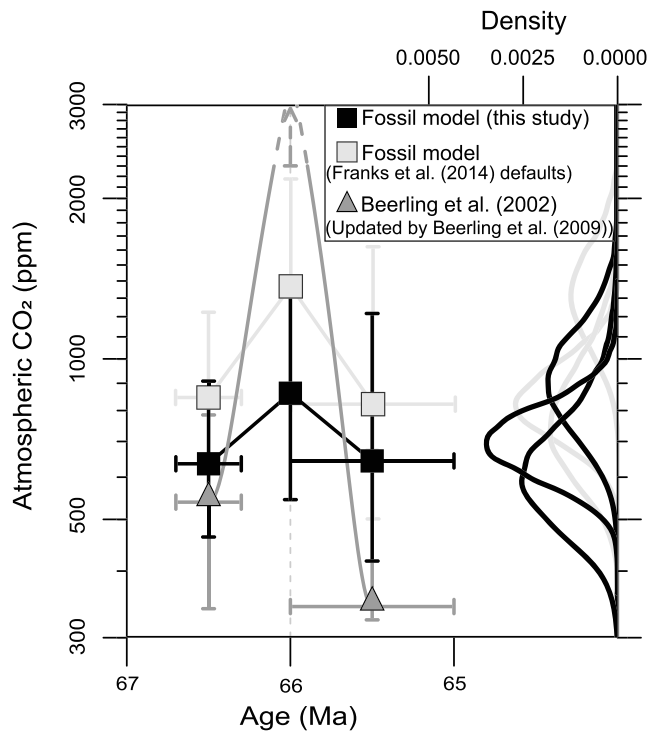


**Figure 3.** Atmospheric CO<sub>2</sub> estimates from the Cretaceous-Paleogene boundary. Estimates from the leaf gas exchange model (this study) are based on the same fossils whose stomatal index was used to estimate CO<sub>2</sub> by Beerling et al. (2002). The gray squares are based on the recommended values from Franks et al. (2014) for assimilation rate and the ratio of operational to maximum stomatal conductance. Error bars represent the 95% confidence interval.

measure them (Table S1). The leaf gas exchange estimate of CO<sub>2</sub> from aff. *Stenochlaena* directly after the K-Pg boundary is 873 ppm (95% confidence interval 550–1,414 ppm). By comparison, the estimates from Beerling et al. (2002; updated by Beerling et al., 2009) are 539 ppm for the Late Cretaceous, >2,300 ppm for the fern layer, and 343 ppm for the early Paleocene.

It is possible that all three of our estimates are falsely high because the model overestimates present-day CO<sub>2</sub> for *G. biloba* (Barclay & Wing, 2016; Kowalczyk et al., 2018; but see Franks et al., 2014) and *S. palustris* at both 500 and 1,000 ppm CO<sub>2</sub> (Figure 1). The relative temporal patterns, though, are more likely to be robust. If we use the generic inputs for  $A_0$  and  $g_{c(op)}/g_{c(max)}$  recommended by Franks et al. (2014), all three estimates increase by ~200–500 ppm (Table S2 and Figure 3), but the increase in CO<sub>2</sub> between the Late Cretaceous and fern layer does not change by very much (+250 ppm) and remains fundamentally different from the original interpretation of Beerling et al. (2002; Figure 3).

A source of uncertainty for the aff. *Stenochlaena* CO<sub>2</sub> estimate is the atmospheric  $\delta^{13}C$  directly at the K-Pg boundary, which affects the calculation of  $c_i/c_a$ . Measured carbon isotopic excursions at the K-Pg boundary range from 0 to  $-3\text{‰}$  (Arens & Jahren, 2000; Beerling et al., 2001; Maruoka et al., 2007; Schimmelmann & DeNiro, 1984; Schulte et al., 2010). Where examined in detail, the excursion in terrestrial sections begins immediately above the K-Pg boundary clay in the fern spike interval, with the most negative values in the early phase of dicot recovery, and a return to preexcursion values no higher than 2–3 m up section (reviewed in Upchurch et al., 2007). For our initial modeling we assume  $-2\text{‰}$  (Text S2). If we instead assume an excursion of  $0\text{‰}$ , comparable to the value at the top of the K-Pg boundary clay, or  $-3\text{‰}$ , the median CO<sub>2</sub> is 1,170 and 762 ppm, respectively. Neither of these changed estimates strongly affect our key interpretations.

Our CO<sub>2</sub> record implies a transient change of ~+250 ppm; if we take the extreme scenario of comparing the lower and upper bounds of the 95% confidence intervals, this change could range from  $-333$  to  $+1,032$  ppm. Critically, we provide the first fully bounded CO<sub>2</sub> estimate from the top of the fern spike interval, and thus likely from within the first 10<sup>3</sup> years after the bolide impact. Our *Ginkgo* estimates bracket the event by roughly 500 kyrs, meaning that we do not know the CO<sub>2</sub> concentration directly before the bolide impact. This is an important deficiency because global temperatures rose ~300 kyrs before the K-Pg boundary and subsequently fell leading up to the boundary (Barnet et al., 2017; Nordt et al., 2003; Petersen et al., 2016; Wilf et al., 2003; Zhang et al., 2018). Zhang et al. (2018) estimate with the pedogenic carbonate proxy a CO<sub>2</sub> concentration of 700 ppm 110 kyrs before the K-Pg boundary (Figure S17), suggesting that Deccan volcanism caused an elevation in CO<sub>2</sub> before the boundary (Courtillot et al., 1986; Tobin et al., 2017, and sources cited within) and therefore the CO<sub>2</sub> spike we report may not be contributed entirely by the bolide-impact.

The Chicxulub bolide impact would release CO<sub>2</sub> almost instantaneously via the vaporization of target carbonate bedrock (Artemieva & Morgan, 2017; O'Keefe & Ahrens, 1989) and wildfires (Durda & Kring, 2004; Wolbach et al., 1990). A recent model for the vaporization of target carbonate bedrock at Chicxulub suggests a modest 54 ppm rise in atmospheric CO<sub>2</sub> (Artemieva & Morgan, 2017). Global wildfires may have caused CO<sub>2</sub> to increase by 315 ppm (Toon et al., 2016), but the extent of these fires is contentious and may have been far less (Belcher, 2009; Belcher et al., 2003, 2004, 2005, 2009, 2015; Harvey et al., 2008; Morgan et al., 2013).

Establishing a link between Deccan volcanism and CO<sub>2</sub> change at the K-Pg boundary is difficult because (1) age uncertainties of the lava flows are on the order of 10<sup>4</sup>–10<sup>5</sup> years (e.g., Renne et al., 2015; Schoene et al., 2015, 2019; Sprain et al., 2019); and (2) constraining the amount and rate of CO<sub>2</sub> release is challenging (Jay &

Widdowson, 2008; Self et al., 2006). Deccan volcanism clearly brackets the K-Pg boundary, but whether there was a pulse of activity within  $10^2$ – $10^3$  years of the boundary is unresolved (Schoene et al., 2019; Sprain et al., 2019). Using existing constraints on the magnitude and pacing of CO<sub>2</sub> release for the Deccan, Tobin et al. (2017) demonstrate that it is possible, in principle, to raise CO<sub>2</sub> concentrations by several hundred parts per million. Future work may provide clarity.

Temperature records spanning the first  $10^2$ – $10^3$  years after the K-Pg boundary are sparse, but most modeling and high-resolution marine data are not consistent with a large change in CO<sub>2</sub>. After a brief “impact winter” (months to decades; Bardeen et al., 2017; Brugger et al., 2017; Taylor et al., 2018; Vellekoop et al., 2014, 2015, 2016), temperatures increased between ~1 and 6 °C depending on paleolatitude and geographic location, with the largest increases often at higher paleolatitudes (MacLeod et al., 2018; Taylor et al., 2018; Vellekoop et al., 2014; Zhang et al., 2018). Terrestrial temperature trends inferred from leaf fossils are somewhat ambiguous and model dependent (Upchurch et al., 2007). Among marine records and most relevant to our study, Taylor et al. (2018) document a 2.5–4 °C warming during the fern spike interval in the southern midlatitudes (present-day New Zealand). Together, these reconstructions best fit a scenario with a modest 1–3 °C rise in global mean surface temperature. If we assume an Earth system sensitivity of 3 °C or higher per CO<sub>2</sub> doubling (Royer, 2016), these records imply—at most—one CO<sub>2</sub> doubling. One exception is a ~5 °C warming within ~100,000 years after the K-Pg boundary at the global stratotype El Kef, Tunisia (~20°N paleolatitude; MacLeod et al., 2018). This subtropical temperature record appears incompatible with our record, suggesting that either CO<sub>2</sub> directly before the K-Pg boundary was substantially lower (<400 ppm) than what our and most other reconstructions imply (Zhang et al., 2018; see also Figure S17) or local changes in ocean chemistry biased the temperature estimates.

In summary, we find no strong evidence for a large pulse of atmospheric CO<sub>2</sub> coincident with the K-Pg boundary. Our CO<sub>2</sub> record from within or directly above the fern spike is most consistent with a CO<sub>2</sub> rise of no more than ~500 ppm and more likely ~250 ppm or less. This is in keeping with the balance of evidence from temperature records and from the carbon cycle modeling of impact vaporization of target bedrock, widespread wildfire, and Deccan volcanism.

#### Acknowledgments

We thank S. Sultan for use of her LI-COR gas exchange analyzer, T. Ku for providing laboratory space, and D. Penman and one anonymous reviewer for helpful comments. Data used in this study are available in the supporting information and Data Set SI.

#### References

- Alroy, J. (2008). Dynamics of origination and extinction in the marine fossil record. *Proceedings of the National Academy of Sciences of the United States of America*, 105(Supplement 1), 11,536–11,542. <https://doi.org/10.1073/pnas.0802597105>
- Archer, D. (2005). Fate of fossil fuel CO<sub>2</sub> in geologic time. *Journal of Geophysical Research*, 110, C09S05. <https://doi.org/10.1029/2004JC002625>
- Arens, N. C., & Jahren, A. H. (2000). Carbon isotope excursion in atmospheric CO<sub>2</sub> at the Cretaceous-Tertiary boundary: Evidence from terrestrial sediments. *PALAIOS*, 15(4), 314–322. [https://doi.org/10.1669/0883-1351\(2000\)015<0314:CIEIAC>2.0.CO;2](https://doi.org/10.1669/0883-1351(2000)015<0314:CIEIAC>2.0.CO;2)
- Artemieva, N., & Morgan, J. (2017). Quantifying the release of climate-active gases by large meteorite impacts with a case study of Chicxulub. *Geophysical Research Letters*, 44, 10–188. <https://doi.org/10.1002/2017GL074879>
- Barclay, R. S., & Wing, S. L. (2016). Improving the *Ginkgo* CO<sub>2</sub> barometer: Implications for the early Cenozoic atmosphere. *Earth and Planetary Science Letters*, 439, 158–171. <https://doi.org/10.1016/j.epsl.2016.01.012>
- Bardeen, C. G., Garcia, R. R., Toon, O. B., & Conley, A. J. (2017). On transient climate change at the Cretaceous-Paleogene boundary due to atmospheric soot injections. *Proceedings of the National Academy of Sciences of the United States of America*, 114(36), E7415–E7424. <https://doi.org/10.1073/pnas.1708980114>
- Barnet, J. S., Littler, K., Kroon, D., Leng, M. J., Westerhold, T., Röhl, U., & Zachos, J. C. (2017). A new high-resolution chronology for the late Maastrichtian warming event: Establishing robust temporal links with the onset of Deccan volcanism. *Geology*, 46(2), 147–150. <https://doi.org/10.1130/G39771.1>
- Beerling, D. J., Fox, A., & Anderson, C. W. (2009). Quantitative uncertainty analyses of ancient atmospheric CO<sub>2</sub> estimates from fossil leaves. *American Journal of Science*, 309(9), 775–787. <https://doi.org/10.2475/09.2009.01>
- Beerling, D. J., Lomax, B. H., Royer, D. L., Upchurch, G. R., & Kump, L. R. (2002). An atmospheric CO<sub>2</sub> reconstruction across the Cretaceous-Tertiary boundary from leaf megafossils. *Proceedings of the National Academy of Sciences of the United States of America*, 99(12), 7836–7840. <https://doi.org/10.1073/pnas.122573099>
- Beerling, D. J., Lomax, B. H., Upchurch, G. R., Nichols, D. J., Pillmore, C. L., Handley, L. L., & Scrimgeour, C. M. (2001). Evidence for the recovery of terrestrial ecosystems ahead of marine primary production following a biotic crisis at the Cretaceous-Tertiary boundary. *Journal of the Geological Society, London*, 158(5), 737–740. <https://doi.org/10.1144/jgs.158.5.737>
- Belcher, C. M. (2009). Reigniting the Cretaceous-Paleogene firestorm debate. *Geology*, 37(12), 1147–1148. <https://doi.org/10.1130/focus122009.1>
- Belcher, C. M., Collinson, M. E., & Scott, A. C. (2005). Constraints on the thermal energy released from the Chicxulub impactor: New evidence from multimethod charcoal analysis. *Journal of the Geological Society, London*, 162(4), 591–602. <https://doi.org/10.1144/0016-764904-104>
- Belcher, C. M., Collinson, M. E., Sweet, A. R., Hildebrand, A. R., & Scott, A. C. (2003). Fireball passes and nothing burns—The role of thermal radiation in the Cretaceous-Tertiary event: Evidence from the charcoal record of North America. *Geology*, 31(12), 1061–1064. <https://doi.org/10.1130/G19989.1>

- Belcher, C. M., Collinson, M. E., Sweet, A. R., Hildebrand, A. R., & Scott, A. C. (2004). Fireball passes and nothing burns—The role of thermal radiation in the Cretaceous-Tertiary event: Evidence from the charcoal record of North America: Comment and reply: Reply. *Geology*, 32(1), e50–e51. <https://doi.org/10.1130/0091-7613-32.1.e51>
- Belcher, C. M., Finch, P., Collinson, M. E., Scott, A. C., & Grassineau, N. V. (2009). Geochemical evidence for combustion of hydrocarbons during the K-T impact event. *Proceedings of the National Academy of Sciences of the United States of America*, 106(11), 4112–4117. <https://doi.org/10.1073/pnas.0813117106>
- Belcher, C. M., Hadden, R. M., Rein, G., Morgan, J. V., Artemieva, N., & Goldin, T. (2015). An experimental assessment of the ignition of forest fuels by the thermal pulse generated by the Cretaceous–Palaeogene impact at Chicxulub. *Journal of the Geological Society, London*, 172(2), 175–185. <https://doi.org/10.1144/jgs2014-082>
- Berry, J. A., & Björkman, O. (1980). Photosynthetic response and adaptation to temperature in higher plants. *Annual Review of Plant Physiology*, 31(1), 491–543. <https://doi.org/10.1146/annurev.pp.31.060180.002423>
- Brugger, J., Feulner, G., & Petri, S. (2017). Baby, it's cold outside: Climate model simulations of the effects of the asteroid impact at the end of the Cretaceous. *Geophysical Research Letters*, 44, 419–427. <https://doi.org/10.1002/2016GL072241>
- Brusatte, S. L., Butler, R. J., Barrett, P. M., Carrano, M. T., Evans, D. C., Lloyd, G. T., et al. (2015). The extinction of the dinosaurs. *Biological Reviews*, 90(2), 628–642. <https://doi.org/10.1111/brv.12128>
- Clyde, W. C., Ramezani, J., Johnson, K. R., Bowring, S. A., & Jones, M. M. (2016). Direct high-precision U–Pb geochronology of the end-Cretaceous extinction and calibration of Paleocene astronomical timescales. *Earth and Planetary Science Letters*, 452, 272–280. <https://doi.org/10.1016/j.epsl.2016.07.041>
- Colbourn, G., Ridgwell, A., & Lenton, T. M. (2015). The time scale of the silicate weathering negative feedback on atmospheric CO<sub>2</sub>. *Global Biogeochemical Cycles*, 29, 583–596. <https://doi.org/10.1002/2014GB005054>
- Courtillot, V., Besse, J., Vandamme, D., Montigny, R., Jaeger, J. J., & Cappetta, H. (1986). Deccan flood basalts at the Cretaceous/Tertiary boundary? *Earth and Planetary Science Letters*, 80(3–4), 361–374. [https://doi.org/10.1016/0012-821X\(86\)90118-4](https://doi.org/10.1016/0012-821X(86)90118-4)
- Doria, G., Royer, D. L., Wolfe, A. P., Fox, A., Westgate, J. A., & Beerling, D. J. (2011). Declining atmospheric CO<sub>2</sub> during the late middle Eocene climate transition. *American Journal of Science*, 311(1), 63–75. <https://doi.org/10.2475/01.2011.03>
- Durda, D. D., & Kring, D. A. (2004). Ignition threshold for impact-generated fires. *Journal of Geophysical Research*, 109, E08004. <https://doi.org/10.1029/2004JE002279>
- Ekart, D. D., Cerling, T. E., Montanez, I. P., & Tabor, N. J. (1999). A 400 million year carbon isotope record of pedogenic carbonate: Implications for paleoatmospheric carbon dioxide. *American Journal of Science*, 299(10), 805–827. <https://doi.org/10.2475/ajs.299.10.805>
- Farquhar, G. D., & Sharkey, T. D. (1982). Stomatal conductance and photosynthesis. *Annual Review of Plant Physiology*, 33(1), 317–345. <https://doi.org/10.1146/annurev.pp.33.060182.001533>
- Franks, P. J., Royer, D. L., Beerling, D. J., Van de Water, P. K., Cantrill, D. J., Barbour, M. M., & Berry, J. A. (2014). New constraints on atmospheric CO<sub>2</sub> concentration for the Phanerozoic. *Geophysical Research Letters*, 41, 4685–4694. <https://doi.org/10.1002/2014GL060457>
- Gradstein, F. M., Ogg, J. G., Schmitz, M., & Ogg, G. (2012). *The geologic time scale 2012*. Amsterdam, The Netherlands: Elsevier.
- Harvey, M. C., Brassell, S. C., Belcher, C. M., & Montanari, A. (2008). Combustion of fossil organic matter at the Cretaceous-Paleogene (K-P) boundary. *Geology*, 36(5), 355–358. <https://doi.org/10.1130/G24646A.1>
- Helliker, B. R., & Richter, S. L. (2008). Subtropical to boreal convergence of tree-leaf temperatures. *Nature*, 454(7203), 511–514. <https://doi.org/10.1038/nature07031>
- Henehan, M. J., Rae, J. W., Foster, G. L., Erez, J., Prentice, K. C., Kucera, M., et al. (2013). Calibration of the boron isotope proxy in the planktonic foraminifera *Globigerinoides ruber* for use in palaeo-CO<sub>2</sub> reconstruction. *Earth and Planetary Science Letters*, 364, 111–122. <https://doi.org/10.1016/j.epsl.2012.12.029>
- Hicks, J. F., Johnson, K. R., Obradovich, J. D., Tauxe, L., & Clark, D. (2002). Magnetostratigraphy and geochronology of the Hell Creek and basal Fort Union Formations of southwestern North Dakota and a recalibration of the age of the Cretaceous-Tertiary boundary. In J. Hartman, K. R. Johnson, & D. J. Nichols (Eds.), *The Hell Creek Formation and the Cretaceous-Tertiary boundary in the northern Great Plains: Geological Society of America Special Paper 361* (pp. 35–55). Boulder, CO: Geological Society of America.
- Hincke, A. J., Broere, T., Kürschner, W. M., Donders, T. H., & Wagner-Cremer, F. (2016). Multi-year leaf-level response to sub-ambient and elevated experimental CO<sub>2</sub> in *Betula nana*. *PLoS ONE*, 11(6), e0157400. <https://doi.org/10.1371/journal.pone.0157400>
- Hönisch, B., & Hemming, N. G. (2005). Surface Ocean pH response to variations in pCO<sub>2</sub> through two full glacial cycles. *Earth and Planetary Science Letters*, 236(1–2), 305–314. <https://doi.org/10.1016/j.epsl.2005.04.027>
- Huang, C., Retallack, G. J., Wang, C., & Huang, Q. (2013). Paleoatmospheric pCO<sub>2</sub> fluctuations across the Cretaceous-Tertiary boundary recorded from paleosol carbonates in NE China. *Palaeogeography, Palaeoclimatology, Palaeoecology*, 385, 95–105. <https://doi.org/10.1016/j.palaeo.2013.01.005>
- Jay, A. E., & Widdowson, M. (2008). Stratigraphy, structure and volcanology of the SE Deccan continental flood basalt province: Implications for eruptive extent and volumes. *Journal of the Geological Society, London*, 165(1), 177–188. <https://doi.org/10.1144/0016-76492006-062>
- Johnson, K. R. (2002). Megafloora of the Hell Creek and lower Fort Union Formations in the western Dakotas: Vegetational response to climate change, the cretaceous-tertiary boundary event, and rapid marine transgression. In J. Hartman, K. R. Johnson, & D. J. Nichols (Eds.), *The Hell Creek Formation and the Cretaceous-Tertiary boundary in the northern Great Plains: Geological Society of America Special Paper 361* (pp. 329–391). Boulder, CO: Geological Society of America. <https://doi.org/10.1130/0-8137-2361-2.329>
- Konrad, W., Katul, G., Roth-Nebelsick, A., & Grein, M. (2017). A reduced order model to analytically infer atmospheric CO<sub>2</sub> concentration from stomatal and climate data. *Advances in Water Resources*, 104, 145–157. <https://doi.org/10.1016/j.advwatres.2017.03.018>
- Konrad, W., Roth-Nebelsick, A., & Grein, M. (2008). Modeling of stomatal density response to atmospheric CO<sub>2</sub>. *Journal of Theoretical Biology*, 253(4), 638–658. <https://doi.org/10.1016/j.jtbi.2008.03.032>
- Kowalczyk, J. B., Royer, D. L., Miller, I. M., Anderson, C. W., Beerling, D. J., Franks, P. J., et al. (2018). Multiple proxy estimates of atmospheric CO<sub>2</sub> from an early Paleocene rainforest. *Paleoceanography and Paleoclimatology*, 13, 1427–1438. <https://doi.org/10.1029/2018PA003356>
- Londoño, L., Royer, D. L., Jaramillo, C., Escobar, J., Foster, D. A., Cárdenas-Rozo, A. L., & Wood, A. (2018). Early Miocene CO<sub>2</sub> estimates from a neotropical fossil assemblage exceed 400 ppm. *American Journal of Botany*, 105(11), 1929–1937. <https://doi.org/10.1002/ajb2.1187>
- MacLeod, K. G., Quinton, P. C., Sepúlveda, J., & Negra, M. H. (2018). Postimpact earliest Paleogene warming shown by fish debris oxygen isotopes (El Kef, Tunisia). *Science*, 360(6396), 1467–1469. <https://doi.org/10.1126/science.aap8525>

- Martínez, C., Gandolfo, M. A., & Cúneo, N. R. (2018). Angiosperm leaves and cuticles from the uppermost cretaceous of Patagonia, biogeographic implications and atmospheric paleo-CO<sub>2</sub> estimates. *Cretaceous Research*, *89*, 107–118. <https://doi.org/10.1016/j.cretres.2018.03.015>
- Maruoka, T., Koeberl, C., & Bohor, B. F. (2007). Carbon isotopic compositions of organic matter across continental Cretaceous–Tertiary (K–T) boundary sections: Implications for paleoenvironment after the K–T impact event. *Earth and Planetary Science Letters*, *253*(1–2), 226–238. <https://doi.org/10.1016/j.epsl.2006.10.028>
- Maxbauer, D. P., Royer, D. L., & LePage, B. A. (2014). High Arctic forests during the middle Eocene supported by moderate levels of atmospheric CO<sub>2</sub>. *Geology*, *42*(12), 1027–1030. <https://doi.org/10.1130/G36014.1>
- McElwain, J. C., Montañez, I., White, J. D., Wilson, J. P., & Yiotis, C. (2016). Was atmospheric CO<sub>2</sub> capped at 1000 ppm over the past 300 million years? *Palaeogeography, Palaeoclimatology, Palaeoecology*, *441*, 653–658. <https://doi.org/10.1016/j.palaeo.2015.10.017>
- McElwain, J. C., & Punyasena, S. W. (2007). Mass extinction events and the plant fossil record. *Trends in Ecology & Evolution*, *22*(10), 548–557. <https://doi.org/10.1016/j.tree.2007.09.003>
- Michaletz, S. T., Weiser, M. D., McDowell, N. G., Zhou, J., Kaspari, M., Helliker, B. R., & Enquist, B. J. (2016). The energetic and carbon economic origins of leaf thermoregulation. *Nature Plants*, *2*(9), 16129. <https://doi.org/10.1038/nplants.2016.129>
- Michaletz, S. T., Weiser, M. D., Zhou, J., Kaspari, M., Helliker, B. R., & Enquist, B. J. (2015). Plant thermoregulation: Energetics, trait-environment interactions, and carbon economics. *Trends in Ecology & Evolution*, *30*(12), 714–724. <https://doi.org/10.1016/j.tree.2015.09.006>
- Montañez, I. P., McElwain, J. C., Poulsen, C. J., White, J. D., DiMichele, W. A., Wilson, J. P., et al. (2016). Climate, pCO<sub>2</sub> and terrestrial carbon cycle linkages during late Palaeozoic glacial–interglacial cycles. *Nature Geoscience*, *9*(11), 824–828. <https://doi.org/10.1038/ngeo2822>
- Montañez, I. P., Norris, R. D., Algeo, T., Chandler, M. A., Johnson, K. R., Kennedy, M. J., et al. (2011). *Understanding Earth's deep past: Lessons for our climate future* (194 pp.). Washington, DC: National Academies Press.
- Morgan, J. V., Artemieva, N., & Goldin, T. (2013). Revisiting wildfires at the K–Pg boundary. *Journal of Geophysical Research: Biogeosciences*, *118*, 1508–1520. <https://doi.org/10.1002/2013JG002428>
- Nordt, L., Atchley, S., & Dworkin, S. (2003). Terrestrial evidence for two greenhouse events in the latest Cretaceous. *GSA Today*, *13*(12), 4–9. [https://doi.org/10.1130/1052-5173\(2003\)013<4:TEFTGE>2.0.CO;2](https://doi.org/10.1130/1052-5173(2003)013<4:TEFTGE>2.0.CO;2)
- O'Keefe, J. D., & Ahrens, T. J. (1989). Impact production of CO<sub>2</sub> by the Cretaceous/Tertiary extinction bolide and the resultant heating of the Earth. *Nature*, *338*(6212), 247–249. <https://doi.org/10.1038/338247a0>
- Pagani, M. (2002). The alkenone-CO<sub>2</sub> proxy and ancient atmospheric carbon dioxide. *Philosophical Transactions of the Royal Society of London A*, *360*(1793), 609–632. <https://doi.org/10.1098/rsta.2001.0959>
- Petersen, S. V., Dutton, A., & Lohmann, K. C. (2016). End-Cretaceous extinction in Antarctica linked to both Deccan volcanism and meteorite impact via climate change. *Nature Communications*, *7*(1), 12079. <https://doi.org/10.1038/ncomms12079>
- Porter, A. S., Gerald, C. E.-F., McElwain, J. C., Yiotis, C., & Elliott-Kingston, C. (2015). How well do you know your growth chambers? Testing for chamber effect using plant traits. *Plant Methods*, *11*(1), 44–40. <https://doi.org/10.1186/s13007-015-0088-0>
- R Core Team (2018). *R: A language and environment for statistical computing*. Vienna, Austria: R Foundation for Statistical Computing. Retrieved from <https://www.r-project.org/>
- Raup, D. M., & Sepkoski, J. J. (1982). Mass extinctions in the marine fossil record. *Science*, *215*(4539), 1501–1503. <https://doi.org/10.1126/science.215.4539.1501>
- Reichgelt, T., D'Andrea, W. J., & Fox, B. R. (2016). Abrupt plant physiological changes in southern New Zealand at the termination of the Mi-1 event reflect shifts in hydroclimate and pCO<sub>2</sub>. *Earth and Planetary Science Letters*, *455*, 115–124. <https://doi.org/10.1016/j.epsl.2016.09.026>
- Renne, P. R., Deino, A. L., Hilgen, F. J., Kuiper, K. F., Mark, D. F., Mitchell, W. S., et al. (2013). Time scales of critical events around the Cretaceous–Paleogene boundary. *Science*, *339*(6120), 684–687. <https://doi.org/10.1126/science.1230492>
- Renne, P. R., Sprain, C. J., Richards, M. A., Self, S., Vanderkluyzen, L., & Pande, K. (2015). State shift in Deccan volcanism at the Cretaceous–Paleogene boundary, possibly induced by impact. *Science*, *350*(6256), 76–78. <https://doi.org/10.1126/science.aac7549>
- Richey, J. D., Upchurch, G. R., Montañez, I. P., Lomax, B. H., Suarez, M. B., Crout, N. M., et al. (2018). Changes in CO<sub>2</sub> during ocean anoxic event 1D indicate similarities to other carbon cycle perturbations. *Earth and Planetary Science Letters*, *491*, 172–182. <https://doi.org/10.1016/j.epsl.2018.03.035>
- Royer, D. L. (2001). Stomatal density and stomatal index as indicators of paleoatmospheric CO<sub>2</sub> concentration. *Review of Palaeobotany and Palynology*, *114*(1–2), 1–28. [https://doi.org/10.1016/S0034-6667\(00\)00074-9](https://doi.org/10.1016/S0034-6667(00)00074-9)
- Royer, D. L. (2014). Atmospheric CO<sub>2</sub> and O<sub>2</sub> during the Phanerozoic: Tools, patterns, and impacts. *Geochemistry Treatise*, *2*, 251–267. <https://doi.org/10.1016/B978-0-08-095975-7.01311-5>
- Royer, D. L. (2016). Climate sensitivity in the geologic past. *Annual Review of Earth and Planetary Sciences*, *44*(1), 277–293. <https://doi.org/10.1146/annurev-earth-100815-024150>
- Royer, D. L., Moynihan, K. M., McKee, M. L., Londoño, L., & Franks, P. J. (2018). Sensitivity of a leaf gas-exchange model for estimating paleoatmospheric CO<sub>2</sub> concentration. *Climate of the Past*, *1*–23. <https://doi.org/10.5194/cp-2018-156>
- Schaller, M. F., Wright, J. D., & Kent, D. V. (2011). Atmospheric pCO<sub>2</sub> perturbations associated with the Central Atlantic Magmatic Province. *Science*, *331*(6023), 1404–1409. <https://doi.org/10.1126/science.1199011>
- Schimmelmann, A., & DeNiro, M. J. (1984). Elemental and stable isotope variations of organic matter from a terrestrial sequence containing the cretaceous/tertiary boundary at York Canyon, New Mexico. *Earth and Planetary Science Letters*, *68*(3), 392–398. [https://doi.org/10.1016/0012-821X\(84\)90124-9](https://doi.org/10.1016/0012-821X(84)90124-9)
- Schoene, B., Eddy, M. P., Samperton, K. M., Keller, C. B., Keller, G., Adatte, T., & Khadri, S. F. R. (2019). U–Pb constraints on pulsed eruption of the Deccan traps across the end-Cretaceous mass extinction. *Science*, *363*(6429), 862–866. <https://doi.org/10.1126/science.aau2422>
- Schoene, B., Samperton, K. M., Eddy, M. P., Keller, G., Adatte, T., Bowring, S. A., et al. (2015). U–Pb geochronology of the Deccan traps and relation to the end-Cretaceous mass extinction. *Science*, *347*(6218), 182–184. <https://doi.org/10.1126/science.aaa0118>
- Schulte, P., Alegret, L., Arenillas, I., Arz, J. A., Barton, P. J., Bown, P. R., et al. (2010). The Chicxulub asteroid impact and mass extinction at the Cretaceous–Paleogene boundary. *Science*, *327*(5970), 1214–1218. <https://doi.org/10.1126/science.1177265>
- Self, S., Widdowson, M., Thordarson, T., & Jay, A. E. (2006). Volatile fluxes during flood basalt eruptions and potential effects on the global environment: A Deccan perspective. *Earth and Planetary Science Letters*, *248*(1–2), 518–532. <https://doi.org/10.1016/j.epsl.2006.05.041>

- Solomon, S., Plattner, G.-K., Knutti, R., & Friedlingstein, P. (2009). Irreversible climate change due to carbon dioxide emissions. *Proceedings of the National Academy of Sciences of the United States of America*, *106*, 1704–1709. <https://doi.org/10.1073/pnas.0812721106>
- Song, X., Barbour, M. M., Saurer, M., & Helliker, B. R. (2011). Examining the large-scale convergence of photosynthesis-weighted tree leaf temperatures through stable oxygen isotope analysis of multiple data sets. *New Phytologist*, *192*(4), 912–924. <https://doi.org/10.1111/j.1469-8137.2011.03851.x>
- Sprain, C. J., Renne, P. R., Vanderkluyzen, L., Pande, K., Self, S., & Mittal, T. (2019). The eruptive tempo of Deccan volcanism in relation to the Cretaceous–Paleogene boundary. *Science*, *363*(6429), 866–870. <https://doi.org/10.1126/science.aav1446>
- Steinthorsdottir, M., Vajda, V., & Pole, M. (2016). Global trends of pCO<sub>2</sub> across the Cretaceous–Paleogene boundary supported by the first Southern Hemisphere stomatal proxy-based pCO<sub>2</sub> reconstruction. *Palaeogeography, Palaeoclimatology, Palaeoecology*, *464*, 143–152. <https://doi.org/10.1016/j.palaeo.2016.04.033>
- Taylor, K. W., Willumsen, P. S., Hollis, C. J., & Pancost, R. D. (2018). South Pacific evidence for the long-term climate impact of the Cretaceous/Paleogene boundary event. *Earth-Science Reviews*, *179*, 287–302. <https://doi.org/10.1016/j.earscirev.2018.02.012>
- Tesfamichael, T., Jacobs, B., Tabor, N., Michel, L., Curran, E., Feseha, M., et al. (2017). Settling the issue of “decoupling” between atmospheric carbon dioxide and global temperature: [CO<sub>2</sub>]<sub>atm</sub> reconstructions across the warming Paleogene–Neogene divide. *Geology*, *45*(11), 999–1002. <https://doi.org/10.1130/G39048.1>
- Tobin, T., Bitz, C., & Archer, D. (2017). Modeling climatic effects of carbon dioxide emissions from Deccan traps volcanic eruptions around the Cretaceous–Paleogene boundary. *Palaeogeography, Palaeoclimatology, Palaeoecology*, *478*, 139–148. <https://doi.org/10.1016/j.palaeo.2016.05.028>
- Toon, O. B., Bardeen, C., & Garcia, R. (2016). Designing global climate and atmospheric chemistry simulations for 1 and 10 km diameter asteroid impacts using the properties of ejecta from the K-Pg impact. *Atmospheric Chemistry and Physics*, *16*(20), 13,185–13,212. <https://doi.org/10.5194/acp-16-13185-2016>
- Upchurch, G. R., Jr., Lomax, B. H., & Beerling, D. J. (2007). Paleobotanical evidence for climatic change across the Cretaceous–Tertiary boundary, North America: Twenty years after Wolfe and Upchurch. In: Jarzen, David M., Manchester, Steven R. Retallack, Gregory J., and Jarzen, Susan A. eds., *Advances in Angiosperm Paleobotany and Paleoclimatic reconstruction: Contributions Honouring David L. Dilcher and Jack A. Wolfe*. Courier Forschungsinstitut Senckenberg 258: 57–74.
- Vajda, V., Raine, J. I., & Hollis, C. J. (2001). Indication of global deforestation at the Cretaceous–Tertiary boundary by New Zealand fern spike. *Science*, *294*(5547), 1700–1702. <https://doi.org/10.1126/science.1064706>
- Vellekoop, J., Esmeray-Senlet, S., Miller, K. G., Browning, J. V., Sluijs, A., & van de Schootbrugge, et al. (2016). Evidence for Cretaceous–Paleogene boundary bolide “impact winter” conditions from New Jersey, USA. *Geology*, *44*(8), 619–622. <https://doi.org/10.1130/G37961.1>
- Vellekoop, J., Sluijs, A., Smit, J., Schouten, S., Weijers, J. W. H., Sinninghe Damsté, J. S., & Brinkhuis, H. (2014). Rapid short-term cooling following the Chicxulub impact at the Cretaceous–Paleogene boundary. *Proceedings of the National Academy of Sciences of the United States of America*, *111*, 7537–7541. <https://doi.org/10.1073/pnas.1319253111>
- Vellekoop, J., Smit, J., van de Schootbrugge, B., Weijers, J. W., Galeotti, S., Damsté, J. S. S., & Brinkhuis, H. (2015). Palynological evidence for prolonged cooling along the Tunisian continental shelf following the K–Pg boundary impact. *Palaeogeography, Palaeoclimatology, Palaeoecology*, *426*, 216–228. <https://doi.org/10.1016/j.palaeo.2015.03.021>
- Wilf, P., Johnson, K. R., & Huber, B. T. (2003). Correlated terrestrial and marine evidence for global climate changes before mass extinction at the Cretaceous–Paleogene boundary. *Proceedings of the National Academy of Sciences of the United States of America*, *100*, 599–604. <https://doi.org/10.1073/pnas.0234701100>
- Wing, S. L., Alroy, J., & Hickey, L. J. (1995). Plant and mammal diversity in the Paleocene to early Eocene of the Bighorn Basin. *Palaeogeography, Palaeoclimatology, Palaeoecology*, *115*(1–4), 117–155. [https://doi.org/10.1016/0031-0182\(94\)00109-L](https://doi.org/10.1016/0031-0182(94)00109-L)
- Wolbach, W. S., Anders, E., & Nazarov, M. A. (1990). Fires at the K/T boundary: Carbon at the Sumbar, Turkmenia, site. *Geochimica et Cosmochimica Acta*, *54*(4), 1133–1146. [https://doi.org/10.1016/0016-7037\(90\)90444-P](https://doi.org/10.1016/0016-7037(90)90444-P)
- Wolfe, A. P., Reyes, A. V., Royer, D. L., Greenwood, D. R., Doria, G., Gagen, M. H., et al. (2017). Middle Eocene CO<sub>2</sub> and climate reconstructed from the sediment fill of a subarctic kimberlite maar. *Geology*, *45*(7), 619–622. <https://doi.org/10.1130/G39002.1>
- Wolfe, J. A., & Upchurch, G. R. (1987). Leaf assemblages across the Cretaceous–Tertiary boundary in the Raton Basin, New Mexico and Colorado. *Proceedings of the National Academy of Sciences of the United States of America*, *84*, 5096–5100. <https://doi.org/10.1073/pnas.84.15.5096>
- Yamori, W., Hikosaka, K., & Way, D. A. (2014). Temperature response of photosynthesis in C<sub>3</sub>, C<sub>4</sub>, and CAM plants: Temperature acclimation and temperature adaptation. *Photosynthesis Research*, *119*(1–2), 101–117. <https://doi.org/10.1007/s11120-013-9874-6>
- Zeebe, R. E. (2013). Time-dependent climate sensitivity and the legacy of anthropogenic greenhouse gas emissions. *Proceedings of the National Academy of Sciences of the United States of America*, *110*, 13,739–13,744. <https://doi.org/10.1073/pnas.1222843110>
- Zeebe, R. E., & Zachos, J. C. (2013). Long-term legacy of massive carbon input to the Earth system: Anthropocene versus Eocene. *Philosophical Transactions of the Royal Society A*, *371*, 1–17. <https://doi.org/10.1098/rsta.2012.0006>
- Zhang, L., Wang, C., Wignall, P. B., Kluge, T., Wan, X., Wang, Q., & Gao, Y. (2018). Deccan volcanism caused coupled pCO<sub>2</sub> and terrestrial temperature rises, and pre-impact extinctions in northern China. *Geology*, *46*(3), 271–274. <https://doi.org/10.1130/G39992.1>

## References From the Supporting Information

- Barral, A., Gomez, B., Legendre, S., & Lécuyer, C. (2017). Evolution of the carbon isotope composition of atmospheric CO<sub>2</sub> throughout the Cretaceous. *Palaeogeography, Palaeoclimatology, Palaeoecology*, *471*, 40–47. <https://doi.org/10.1016/j.palaeo.2017.01.034>
- Breecker, D., & Retallack, G. (2014). Refining the pedogenic carbonate atmospheric CO<sub>2</sub> proxy and application to Miocene CO<sub>2</sub>. *Palaeogeography, Palaeoclimatology, Palaeoecology*, *406*, 1–8. <https://doi.org/10.1016/j.palaeo.2014.04.012>
- Breecker, D. O., Sharp, Z. D., & McFadden, L. D. (2009). Seasonal bias in the formation and stable isotopic composition of pedogenic carbonate in modern soils from central New Mexico, USA. *Geological Society of America Bulletin*, *121*(3–4), 630–640. <https://doi.org/10.1130/B26413.1>
- Gardner, R. O. (1975). An overview of botanical clearing technique. *Stain Technology*, *50*(2), 99–105. <https://doi.org/10.3109/10520297509117042>
- Leslie, C. E., Peppe, D. J., Williamson, T. E., Heizler, M., Jackson, M., Atchley, S. C., et al. (2018). Revised age constraints for Late Cretaceous to early Paleocene terrestrial strata from the Dawson Creek section, Big Bend National Park, west Texas. *Geological Society of America Bulletin*, *130*(7–8), 1143–1163. <https://doi.org/10.1130/B31785.1>

- Nordt, L., Atchley, S., & Dworkin, S. (2002). Paleosol barometer indicates extreme fluctuations in atmospheric CO<sub>2</sub> across the cretaceous-tertiary boundary. *Geology*, *30*(8), 703–706. [https://doi.org/10.1130/0091-7613\(2002\)030<0703:PBIEFI>2.0.CO;2](https://doi.org/10.1130/0091-7613(2002)030<0703:PBIEFI>2.0.CO;2)
- Royer, D. L., & Hren, M. T. (2017). Carbon isotopic fractionation between whole leaves and cuticle. *PALAIOS*, *32*(4), 199–205. <https://doi.org/10.2110/palo.2016.073>
- Tipple, B. J., Meyers, S. R., & Pagani, M. (2010). Carbon isotope ratio of Cenozoic CO<sub>2</sub>: A comparative evaluation of available geochemical proxies. *Paleoceanography*, *25*, PA3202. <https://doi.org/10.1029/2009PA001851>
- Zhang, K., Zhao, Y., & Guo, X. (2011). Conifer stomata analysis in paleoecological studies on the Loess Plateau: An example from Tianchi Lake, Liupan Mountains. *Journal of Arid Environments*, *75*(11), 1209–1213. <https://doi.org/10.1016/j.jaridenv.2011.04.023>